J Ther Eng, Vol. 8, No. 2, pp. 202–220, March 2022

Journal of Thermal Engineering
Web page info: https://jten.yildiz.edu.tr
DOI: 10.18186/thermal.1078957

Journal of Thermal Engineering

Research Article

Performance estimation of a solar chimney power plant (SCPP) in several regions of Turkey

Khaoula IKHLEF[1,*], İbrahim ÜÇGÜL[2], Salah LARBI[1], Samir OUCHENE[1]

[1]Mechanical Engineering Department, GMD laboratory, Polytechnic National School (ENP), B.P. 182, El-Harrach, Algiers, Algeria
[2]YEKARUM Laboratory, Süleyman Demirel University (SDU), 32260, Merkezi, Isparta, Turkey

ARTICLE INFO

Article history
Received: 29 August 2020
Accepted: 7 January 2021

Keywords:
Solar Chimney Power Plant (SCPP), Storage system, Turkey meteorological data, Numerical study

ABSTRACT

As the demand for energy increases, it will be more and more necessary for Turkey to diversify its energy sources by investing in renewable energy technologies. In this study, we have presented an updated review of solar chimney power plants, including most analytical, experimental, and numerical simulation studies. We have also analyzed the effect of environmental factors on the performance of a large/small scale prototype of a solar chimney with a thermal storage system for different meteorological data. We have considered five regions of Turkey corresponding to different weather conditions (Adana, Antalya, Burdur, Isparta, and Izmir). The small-scale prototype's theoretical results were compared with the solar chimney prototype's experimental data acquired at the Suleyman Demirel University. Good agreement is observed between theoretical and experimental results. The obtained results showed that the global horizontal irradiance, the temperature, the relative humidity, and the wind velocity influence the power output. Antalya region has the best power production according to it is the warmest and most irradiating site. Notice that the total annual power produced is 46.34E+6 kWh and 439.1E+3 kWh for large and small prototypes, respectively. The high wind velocity of the region generates a decrease in power production.

Cite this article as: Khaoula I, İbrahim Ü, Salah L, Samir O. Performance estimation of a solar chimney power plant (SCPP) in several regions of Turkey. J Ther Eng 2022;8(2):202–220.

INTRODUCTION

Solar chimney power plant is a renewable energy technology for electric power production. It consists of three main components (Figure. 1), the collector, the turbine, and the chimney tower.

In the collector, the solar energy is transformed into thermal energy. However, in the chimney tower, the produced thermal energy is first turned into kinetic energy then finally into electric power through wind turbines and

***Corresponding author.**
*E-mail address: khaoula.ikhlef@g.enp.edu.dz, ibrahimucgul@sdu.edu.tr, salah.larbi@g.enp.edu.dz, samir.ouchene@g.enp.edu.dz

This paper was recommended for publication in revised form by Regional Editor Jaap Hoffman

Published by Yıldız Technical University Press, İstanbul, Turkey

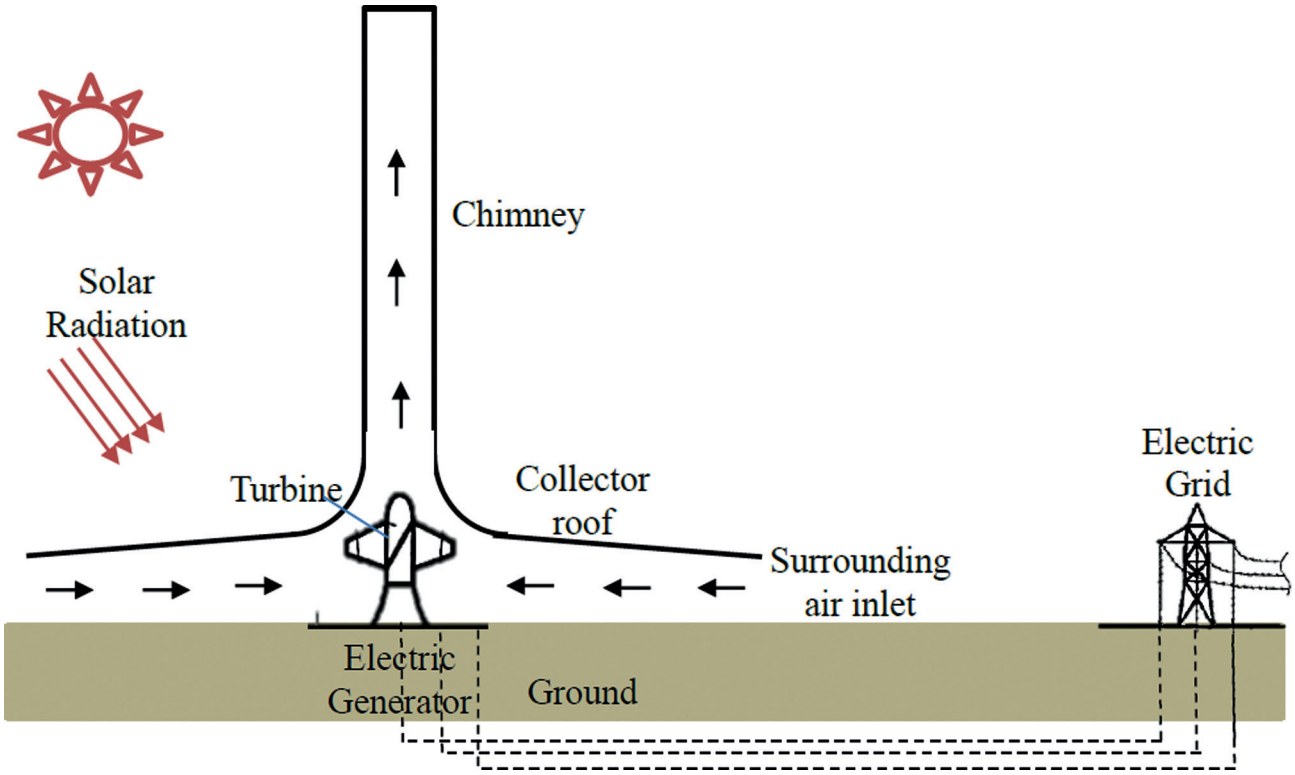

Figure 1. Components of the solar chimney power plant. Modified from Kasaeian et al. [1]

generators. The system includes specific natural impacts and forces (greenhouse effect, chimney effect, Venturi effect, Coriolis force). The technology is reliable, simplistic, and convenient for developing countries, which are sunny and usually have insufficient natural material resources. Economic evaluations based on experience and expertise have confirmed that SCPPs can provide electricity at comparable prices to traditional power plants. Researchers have previously found that electricity costs vary between 0.010 € / kWh and 0.037 € / kWh [2].

Schlaich can be considered as the pioneer in the field of solar chimney power plant technology. Indeed, he presented SCPP technology in a congress in 1978 [3] to design and subsequently build, with his teammates, the prototype of a SCPP in Manzanares, Spain. The prototype had 194.6 m in height [4], a collector diameter of 244 m. Only one turbine with four blades is vertically oriented and placed at the tower's bottom. The prototype was performed and operated until 1989 by producing a maximum power of 50 kW [5]. The feasibility and practicability of the SCPP have been checked throughout its generating life. Later on, numerical, analytical, and experimental research have been performed to understand the efficiency of the SCPP to build a prototype achieving the best performance in energy generation.

Different experimental purposes have been successfully created, developed, and examined in the last decade in which constructions differ from one installation to another. Figure 2 illustrates some SCPP. Notice that the basic prototype of a SCPP was that of Manzanares in Spain, consisting of a metal tower 0.00125 m thick and a PVC roof collector [6]. This prototype was created to collect measurements on the thermal and dynamic fields. In 1985, Kulunk [7] managed to produce 0.14 W of electricity from a scaled-down system, a 2 m tower heigh, and a 9 m^2 collector area, in Izmit, Turkey. In 1997, a prototype of a solar chimney was created by Pasurmarthi and Sherif in Florida [8] (Figure 2. (a)), with a pilot installation of a 7.92 m conical tower and a collector diameter of 9.15 m. In 2002, a SCPP (Figure 2. (b)) constructed in Wuhan in China, is composed of a collector 10 m in diameter and a tower 8 m in high [9]. It was modified several times. The latest structure consisted of a 4.8 mm thick glass cover collector and a PVC tower (Figure 2. (c)). Based on the necessity for facilities for long-term power plans, the Botswana Ministry of Science and Technology has invented and constructed a facility for examination [10].

Another prototype was constructed with the dimensions of 11 m tower high and a 1 m collector diameter

(Figure 2. (d)); this installation was built in the university of Federal de Minas Gerais in Brazil [11]. The tower was an assemblage of 5 wooden modules of cylindrical shape. Each one had a high of 2.2 m, covered inside and outside with glass fibers. The collector diameter was 25 m, and 0.5 m manufactured adopting a plastic film carried by tubular steel construction. Another installation of a solar chimney was built in Isparta, Turkey, in the laboratory of Suleyman Demirel University [12], with a 15 m high and a 16 m diameter collector (Figure 2. (e)). In 2002, Golder created a small prototype of the solar chimney in the laboratory of RMIT University, Australia [13]. The researcher assembled the combination of a solar basin of 1.85 m in-depth, 4.2 m in diameter, and a tower of 8 m in height, 0.35 m in diameter (Figure 2. (f)).

In 2011, the NIT Hamirpur campus constructed a small-scale SCPP composed of a collector of a diameter of 1.4 m and an 80 cm height tower by Mehla and his associates in India [14]. The study registered that the SCPP prototype with 8 cm in tower diameter achieved the highest velocity at the ratio of tower diameter to tower height was 0.1. Bugutekin [15] built a SCPP in Turkey to understand the temperature's impact and the collector diameter on the chimney tower's airflow rate towers rate towers airflow rate. The returns displayed that the ground temperature progressed with the addition of the collector area, and so, their temperature and airflow rate at the bottom of the tower increased immediately. In 2012, Al-Dabbas [16] built the first pilot SCPP in Jordan. He was interested in estimating airflow velocity, solar radiation, temperature, and voltage variation. Chappell et al. [17] created a small prototype of SCPP to attain less expensive elements and maintenance exertion without the exploitation of large devices. In 2020, Nasraoui and his collaborators [18] created a solar chimney prototype and studied the divergent chimney shape's effect on airflow behavior. They found that the chimney's developed divergence shape was more powerful and more efficient and directly affected the efficiency of the SCPP prototype. Azizi et al. [19] built and installed a prototype of SCPP in Algeria to collect results to encourage the government to invest in this area. They found that the air velocity and the collectors' temperature reached 3.1 m/s and 63 °C, respectively, knowing that the meteorological data were 994 W/m^2 for solar irradiance and 40.5 °C for the ambient temperature.

Fundamental studies of the Manzanares power plant prototype carried out by Haaf et al. [6] displayed an examination of the power balance, design models, and study of the system's cost of energy production. Since then, considerable efforts were developed to size and estimate the power production of SCPP to confirm their availability and utility. Padki et al. [20] analyzed the viability of generating electricity from medium to large-scale solar chimneys, in addition to research on the possibilities of supplying rural areas with electricity. Schlaich et al. [21] presented a reproach on the possibility of exploiting the experimental data from the Manzanares prototype to predict the characteristics of larger installations ranging from 5-30 MW up to 100 MW. Chergui et al. [22] demonstrated in their investigation on SCPP in a southwestern region of Algeria the importance of the Adrar region as an attractive site for solar thermal power production. Larbi et al. [23] presented an analysis of the energy performance of a SCPP planned to supply electrical energy to isolated villages located in the southwestern district of Algeria. The authors focused on the city of Adrar, where solar radiation is essential. The obtained results proved that the SCPP could generate an average of 140 to 200 kW of power in the year. Ikhlef and Larbi [24] conducted a study to predict the performance analysis of SCPP with and without a thermal storage system. The obtained results showed the influence of meteorological conditions, the thermal storage system, and geometrical parameters on power production.

As a research of mathematical models, we introduce the following studies. Padki and Sherif [25] suggested a single analytical model for predicting the production of a SCPP with an error of 6% compared to predictions. The mathematical model composed of the equations of continuity, conservation of the movement's momentum, and energy was governing the one-dimensional flow of hot air in the solar chimney tower. Li and his collaborators [26] developed a theoretical hourly model to identify the chimney's influence and the collector on the energy generation using the Sinkiang meteorological data in China. Bernardes and his teammates [27] manifested a numerical model for the one-dimensional airflow in a solar chimney, describing its energy behavior via estimating the power produced under the different construction conditions, operation, and environment. In another study [28], they reported a theoretical analysis of a SCPP based on a laminar natural convection understudy state regime. The technic of finite volumes is used in solving the mathematical model in generalized coordinates.

Zhou et al. [29] conducted a numerical study on the performance of a SCPP based on Navier-Stokes equations. The results showed that the simulated temperature field and the flow field were in agreement with the measurements. The maximum average temperatures are located at 0-5 to 3-5 m from the collector's center. Maia et al. [30] achieved statistical research of the turbulent and transient airflow through a SCPP utilizing the finite volume method (FVM) in generalized coordinates to determine the conservation and transport equations to evaluate the influence of geometric parameters, as well as the materials used in the performance of a SCPP. The demonstration showed that the mass flow increased with the increasing height and diameter of the tower. The authors demonstrated that those two parameters represented the most important physical parameters in designing a SCPP. Chergui et al. [31] developed a digital CFD code, and it was validated by Vahl Davis Benchmark

(a) Modified from Sherif et al. [8]

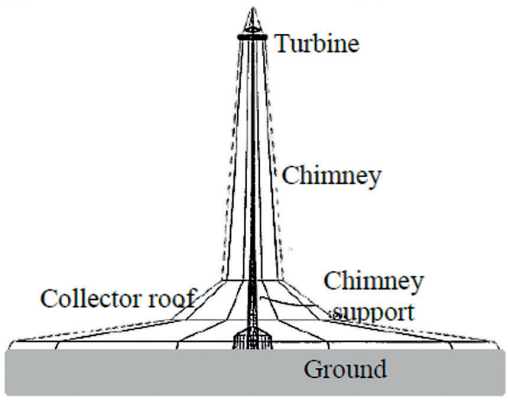

(b) Modified from Zhou et al. [9]

(c) Modified from Botswana et al. [10]

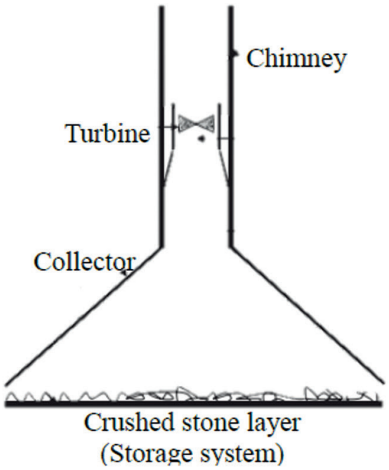

(d) Modified from Ferreira et al. [11]

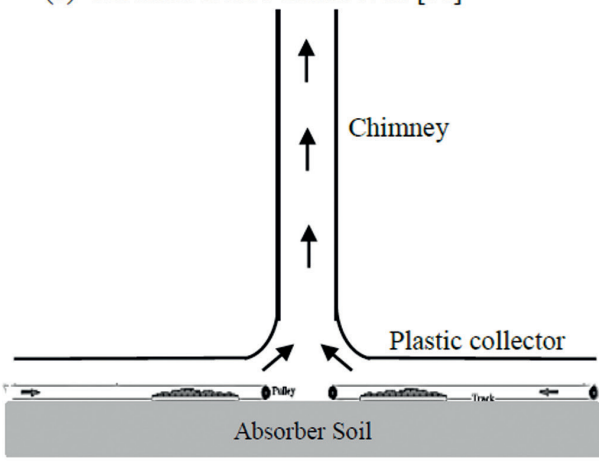

(e) Modified from Koyun et al. [12]

(f) Modified from Golder [13]

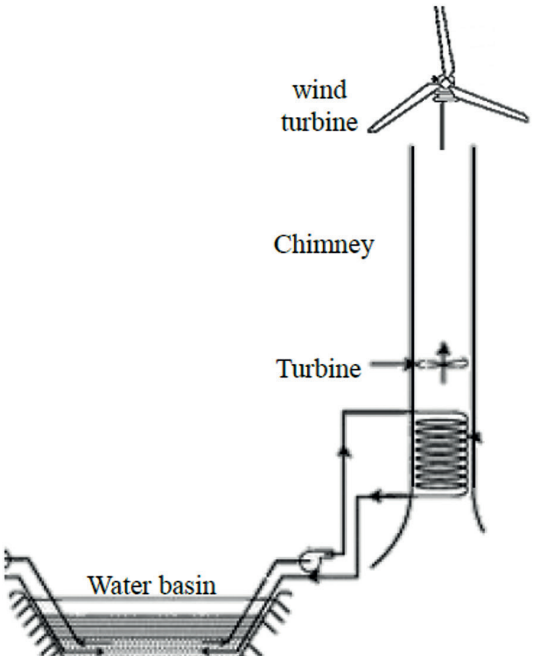

Figure 2. Schematic diagrams and pictures of some prototypes of SCPP.

testing solutions of natural convection. Performance studies related to geometric and operational parameters have been carried out.

Similar studies prior to this one was performed. Indeed, the study carried out by Bugutekin [15] aimed to determine the effect of temperature, airflow rate, and other parameters on the energy production of a solar chimney prototype. For this purpose, at certain times of the day, airflow rate and temperature in the chimney, ambient air velocity, ambient temperature, surface temperature of the collector, and solar radiation values were measured and evaluated. The author noticed the effect of weather conditions such as wind speed on system output. Taybi et al. [32] presented a study whose aim was to examine the effect of varying meteorological conditions such as solar radiation and ambient temperature to estimate a solar chimney's performance theoretically. Zhou et al. [33] investigated the influence of temperature on a large-scale SCPP's performance by taking the daily ambient temperature profile with one peak and the diurnal ambient temperature range. Compared to the solar radiation intensity and humidity, the diurnal ambient temperature range was a good factor in the power plant output's daily profile.

Chandramohan and Das [34] presented a 3D study on the effect of ambient temperature, solar flux, wind flow, and other parameters on a solar chimney's performance. The temperature change range was 293-318 K, while the solar flux change range was 293-900 W / m^2. They found that the maximum overall efficiency was reached when irradiation was at least 900 W / m^2. Finally, in the study presented by Al-Dabbas [16], the goal was to build and evaluate Jordan's solar chimney prototype. He concluded that the power generation capacity depends on solar irradiance, ambient temperature, and other meteorological parameters.

In this study, we have investigated numerically the performance of a SCPP with a thermal storage system for large/small scale power plants using the Bernardes model. The analysis was based on different parameters such as the temperature, the incident solar radiation, the humidity, and the wind velocity by considering other factors as fixed values such as the transmissivity, the emissivity, the absorptivity of the collector, and the turbine efficiency. The study is carried out for different Turkey regions (Adana, Antalya, Burdur, Isparta, and Izmir).

MATHEMATICAL MODEL

The mathematical model is based on conservative balance equations in the different components of the solar chimney by considering the fluid flow as incompressible and viscous in the SCPP. The study aims to analyze the one-dimensional fluid flow and heat transfer in large/small scale SCPP prototypes using the Bernardes model [27, 35-37] and the Pretorius' model [38]. The energy output depends on different characteristics such as the ambient conditions (Irradiation, temperature, humidity, and wind speed) and the design of the installation (dimensions of the chimney, collector, and storage system). The height collector roof is kept inversely proportional to the power plant centerline's distance to preserve the average radial airspeed constant along with the collector.

Collector

The temperature increase in the collector part is delimited in this part. This study was achieved by considering the first mass flow rate while calculating the absolute value using iterative procedures. The collector studied a cavity between two parallel plates [39, 40].

The reported analysis using Bernardes models is based on the next hypotheses [27, 37]:

Continuity equation

- One-dimensional radial flow;
- No regular heating of the collector area in expressions of the sun's altitude angle ignored; the air in the collector is considered as axisymmetric flow;
- The roof of the collector is inclined from the outer boundary towards the tower;
- Unsteady state conditions;
- Flow in collector is examined as a flow between two parallel plates;
- Collector is placed over an unattractive surface;
- Humid flowing air is considered a combination of two ideal gases.

The simplified equation is given as [37]:

$$\frac{1}{r}\frac{\partial}{\partial r}\left(\rho v r H\right)=0 \tag{1}$$

Momentum equation

$$-\left(H\frac{\partial p}{\partial r}+\tau_r+\tau_g+\frac{F_{supports}}{r\Delta\theta}\right)=\rho v H\frac{\partial v}{\partial r} \tag{2}$$

Energy equation

- An increase in collector height across the length of the radial control was ignored;
- Unsteady state conditions;
- Transient kinetic energy terms, Radial conduction, and kinetic energy are negligible;
- Heat transfer in the ground: transient heat conduction in semi-infinite solid.

Roof energy equation [38]:

$$\alpha_{eb}I_{hb}+\alpha_{ed}I_{hd}+q_{gr}=q_{ra}+q_{rs}+q_{rh} \tag{3}$$

Such as:

The radiation heat flux from the ground to the collector roof is presented as [38]:

$$q_{gr} = F_{gr}\sigma\left(T_g^4 - T_r^4\right) \tag{4a}$$

$$q_{gr} = h_{gr}\left(T_g - T_r\right) \tag{4b}$$

The convection heat flux from the collector roof to the ambient air is given by [38]:

$$\boldsymbol{q_{ra}} = \boldsymbol{h_{ra}}\left(\boldsymbol{T_r} - \boldsymbol{T_a}\right) \tag{5}$$

The energy lost by heat flux radiation from the collector roof to the sky can be expressed as [38]:

$$q_{rs} = \epsilon_r\left(T_r^4 - T_{sky}^4\right) \tag{6a}$$

$$q_{rs} = h_{rs}\left(T_r - T_{sky}\right) \tag{6b}$$

The convection heat flux from the collector roof to the air in the collector is expressed as [38]:

$$q_{rh} = h_{rh}\left(T_r - T\right) \tag{7}$$

Ground energy equation [38]:

$$z = 0\,(Ground\ surface)\ \ \left(\tau_e\alpha_g\right)_b I_{hb} + \left(\tau_e\alpha_g\right)_d I_{hd} = q_{gr} - k_g\left.\frac{\partial T_g}{\partial z}\right|_{z=0} + q_{gh} \tag{8}$$

$$z > 0\ \ -k_g\frac{\partial^2 T_g}{\partial z^2} + \rho_g c_{pg}\frac{\partial T_g}{\partial t} = 0 \tag{9}$$

$$z = \infty\ \ \frac{\partial T_g}{\partial z} = 0 \tag{10}$$

Air equation [38]:

$$q_{rh} + q_{gh} = \rho\upsilon H\frac{\partial}{\partial r}\left(c_p T\right) \tag{11}$$

Chimney

The tower or the chimney transforms the thermal power provided by the collector into kinetic energy. The density variation generated by the growth in temperature in the collector operates as the driving power. It is assumed that the heat transfer on the surface of the fireplace piece is negligible. By adopting the simplifications used in [27, 37], we obtain:

Continuity equation

$$\frac{\partial}{\partial z}\left(\rho_c\upsilon_c\right) = 0 \tag{12}$$

Momentum equation
- Area always stresses overall control volume;
- Purely axial flow;
- Unsteady state conditions.

$$-\frac{\partial p_c}{\partial z} - \left(\frac{\tau_c\pi d_c + F_{bw}}{A_c}\right) = \rho_c\left(g + \upsilon_c\frac{\partial\upsilon_c}{\partial z}\right) \tag{13}$$

Energy equation
- Radial conduction, transient kinetic energy terms, and kinetic energy are negligible;
- Unsteady state conditions;
- Heat losses into the wall of the chimney are neglected.

The energy equation in the chimney is [37]:

$$RT_c\frac{\partial}{\partial z}\left(\rho_c\upsilon_c\right) + \rho_c\upsilon_c\left(c_{pc}T_c\right) + \frac{\partial}{\partial z}\left(\rho_c\upsilon_c gz\right) = 0 \tag{14}$$

The impact of humidity is introduced into the density equation in the chimney, which is given by [41]:

$$\rho_c = \frac{1}{R_A T}\left[P - \left(1 - \frac{R_A}{R_V}\right)\varphi P_s(T)\right] \tag{15}$$

$P_S(T)$ is the saturation vapor pressure obtained from reference [42].

Turbine and Generator

The heat flow generated by the collector is turned into kinetic energy and potential energy through the chimney. Thus, the density variation of the air induced by the temperature increase in the collector act as managing energy. The chimney base, which is the outflow of the collector, is linked to the surrounding atmosphere. Between the tower base (collector outlet) and the surroundings, a pressure variation Δptot is delivered. The relevant governing equations assumptions for the turbine are [27, 37]:

Momentum equation
- Static and dynamic pressure was taken into consideration.

Energy equation
- Temperature drops across the turbine.

The theoretical power using by the turbine is given as [37]:

$$P = \Delta p_{tot} A_c w_{tot}\eta_t x\sqrt{1-x} \tag{16}$$

Figure 3 illustrates the flowchart used for the computer program developed in this study.

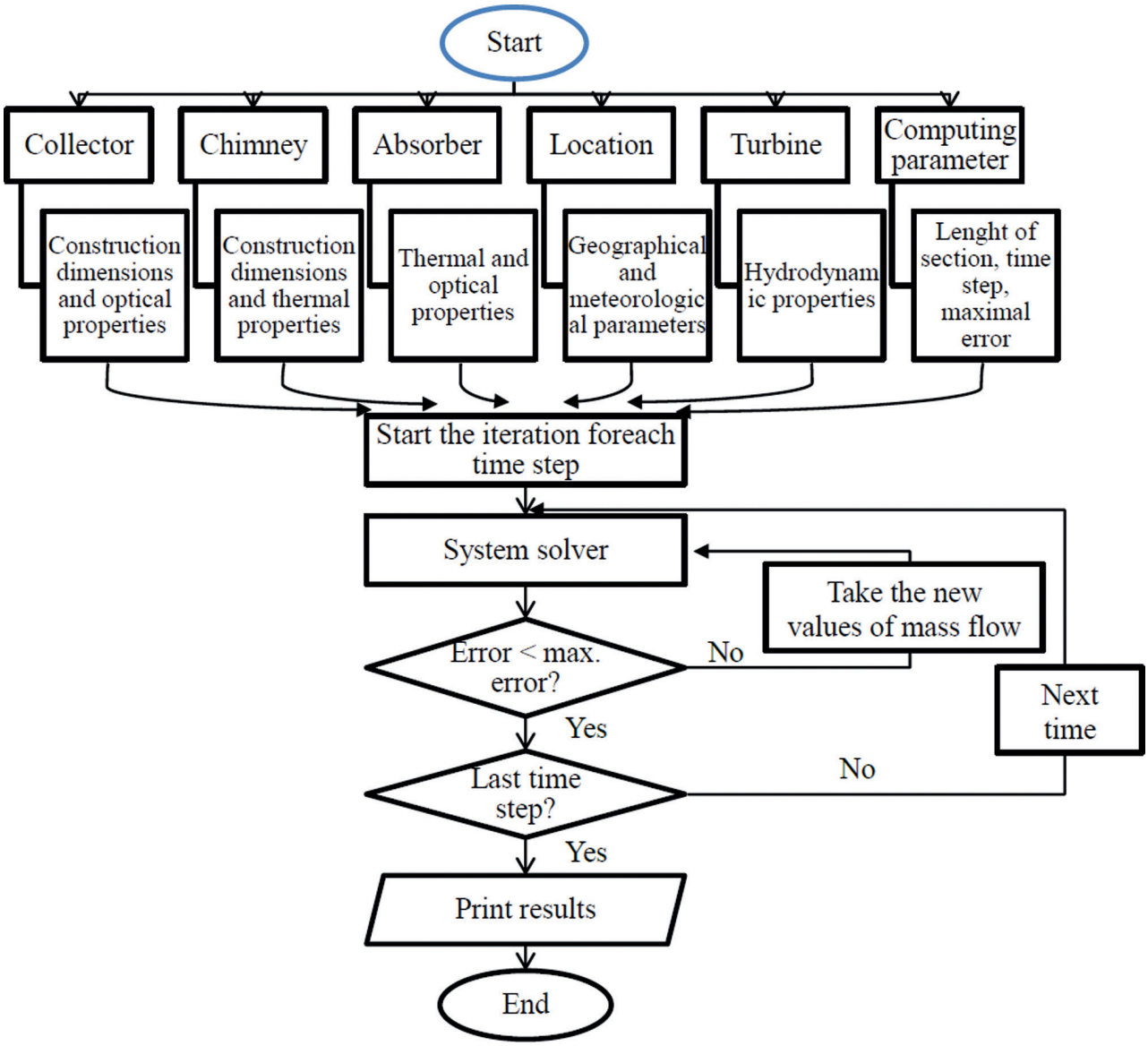

Figure 3. The algorithm used for the numerical simulation in the computer program. Modified from Dos Santos Bernardes [27].

NUMERICAL SIMULATION

The finite difference method was used to solve the mathematical model. A computer simulation program using Java language has been developed to solve the mathematical model [43]. Such as the program used to determine the mass flow rate through the prototype, which will maximize the plant's power output at a given time and register the performance of the solar chimney.

VALIDATION

Before presenting the different results obtained in this study, we expect to validate our numerical results. For this, and using the mathematical model described previously, we simulated the performance of the small-scale prototype of a specific day (August 15, 2004), and we have compared the theoretical results calculated with the experimental ones obtained on a solar chimney prototype installed at the Süleyman Demirel University SDU.

The experimental data were imported from the project (TPD Project No: 2003K121020) [44, 45]. The installation was carried out by a group of researchers in SDU-YEKARUM and supported by the State Planning Organization (TPD). The SCPP prototype had 16 m for the collector's diameter and 15 m for the chimney's height. These configurations are the same as the small-scale theoretical prototype's inputs.

The obtained numerical results were compared with the experimental ones. Table 1 shows the comparison between the theoretically acquired solar radiation results with experimental data and EIE data. Figure 4 presents the comparison of the results between the small-scale prototype's experimental and theoretical output powers.

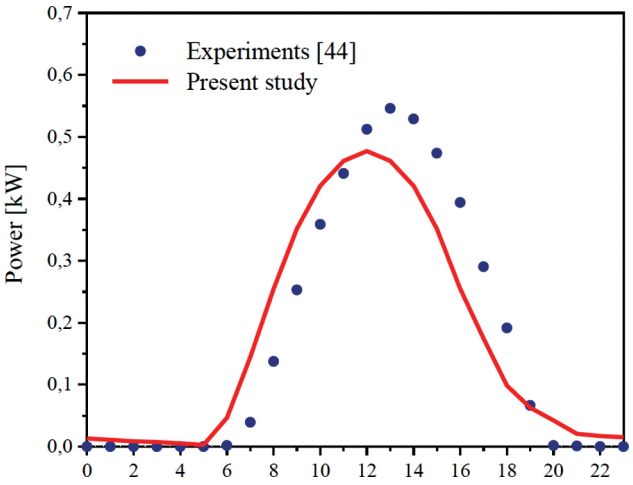

Figure 4. Output power versus time in hours for August 15. Results comparison.

Remember that the solar radiation related to the theoretical results is derived from the mathematical model used by not considering the cloud effects on solar radiation propagation. Experimental data were obtained at the site of Süleyman Demirel University, SDU, while the values of EIE are supplied by the meteorological station service, which is quite far from SDU.

According to these results, there is a cooperative agreement between the calculated theoretical results and the experimental data. The results values are very close to each other at certain times, while they changed slightly at other times. One of the reasons for these different results is that the measurements were taken in a region other than where the solar chimney is located. Another reason is due to the day of measurement when the ambient air temperature and solar irradiation were higher than the theoretical inputs [45].

Table 1 shows the theoretical and experimental GHIs. We notice that from 12:00 to 20:00, the experimental GHI values are more significant than the theoretical ones, which explains the difference between the curves in figure 4 at this period of time.

Table 1. Solar radiation values collected from 3 sources for the day, August 15, 2004

	GHI [W/m²]		
Hours	**Theoretical [W/m²]**	**Experimental [W/m²] [44]**	**Value of EIE [W/m²] [44]**
01:00	0	0	0
02:00	0	0	0
03:00	0	0	0
04:00	0	0	0
05:00	1,06667	0	0
06:00	49,4667	3	38.2
07:00	252	66	218.2
08:00	432,333	231	392.3
09:00	593,033	425	589.1
10:00	735,167	603	758
11:00	829,633	741	888
12:00	762,333	861	937
13:00	755,633	938	568.5
14:00	724,5	889	417.7
15:00	671,3	796	553.8
16:00	530,733	662	478.4
17:00	374,233	488	443.7
18:00	215,033	322	160.8
19:00	75,3333	112	15.3
20:00	0,666667	3	0
21:00	0	0	0
22:00	0	0	0
23:00	0	0	0

RESULTS AND DISCUSSIONS

The numerical simulation procedure is applied to the small and the large solar chimney prototype through an iterative process where the air temperature, the mass flow, the heat transfer coefficients, the friction losses, the drag losses, and the pressure potential have included as parameters in the simulation. In the model presented previously, the meteorological data were obtained using the METEONORM 7 software database, and an hourly time step was selected by taking the standard TMY3 format.

To achieve this goal, we considered two prototypes of solar chimneys (large-scale and small-scale) to estimate

Table 2. Input data used in the numerical simulation

	Small prototype	Large prototype	Units
Collector input data			
Collector diameter	16	300	[m]
Collector useful length	7.40	138.7	[m]
Roof shape exponent	1		[-]
Roof inlet height	0.65	3	[m]
Number of volumes for the collector:	10	100	[-]
Support diameter	0.12		[m]
Support drag coefficient	1		[-]
Support tangential pitch	1.5	15	[m]
Support radial pitch	1.5	15	[m]
Inlet loss coefficient	1		[-]
Emissivity of glass	0.87		[-]
Absorber emissivity	0.90		[-]
Refractive index of glass	1.52		[-]
Extinction coefficient of glass	4		[1/m]
Thickness of glass	0.004		[m]
Chimney input data			
Chimney diameter	1.2	16	[m]
Chimney base height	0.65	8	[m]
Chimney height	15	194.6	[m]
Inside wall roughness	0.002		[-]
Ring stiffener drag coefficient	0.025		[-]
Number of ring stiffeners	4		[-]
Turbine inlet loss coefficient	0.14		[-]
Turbo-generator efficiency	0.80		[-]
x-factor	0.50		[-]
Ground/Storage data			
Depth of ground	1		[m]
Number of volumes (water):	16	60	[m]
Thermal conductivity of the ground	1.83		[W/m K]
Density of ground	2160		[kg/m^3]
Specific heat capacity of the ground	710		[J/kg K]
Absorptivity of ground	0.90		[-]
Layer thickness	0.10		[m]
Volumes for the layer	16	60	[-]
Layer thermal conductivity	0.613		[W/m K]
Layer density:	995.7		[kg/m^3]
Layer specific heat capacity (Gypsum)	4179		[J/kg K]

Table 3. Climate data for selected regions of Turkey

	Adana	Antalya	Burdur	Isparta	Izmir
Latitude (°N)	37.0	36.9	37.7	37.8	38.4
Longitude (°E)	35.3	30.7	30.3	30.6	30.7
Elevation (m)	20	50	952	997	25
Average annual DNI (W/m²/year)	1319	2193	1775	1781	1981
Average annual GHI (W/m²/year)	1533	1895	1660	1652	1768
Ambient temperature (°C)	19.2	19.4	12.5	12.5	17
Wind speed (m/s)	2.5	4.2	1.7	1.7	4.3

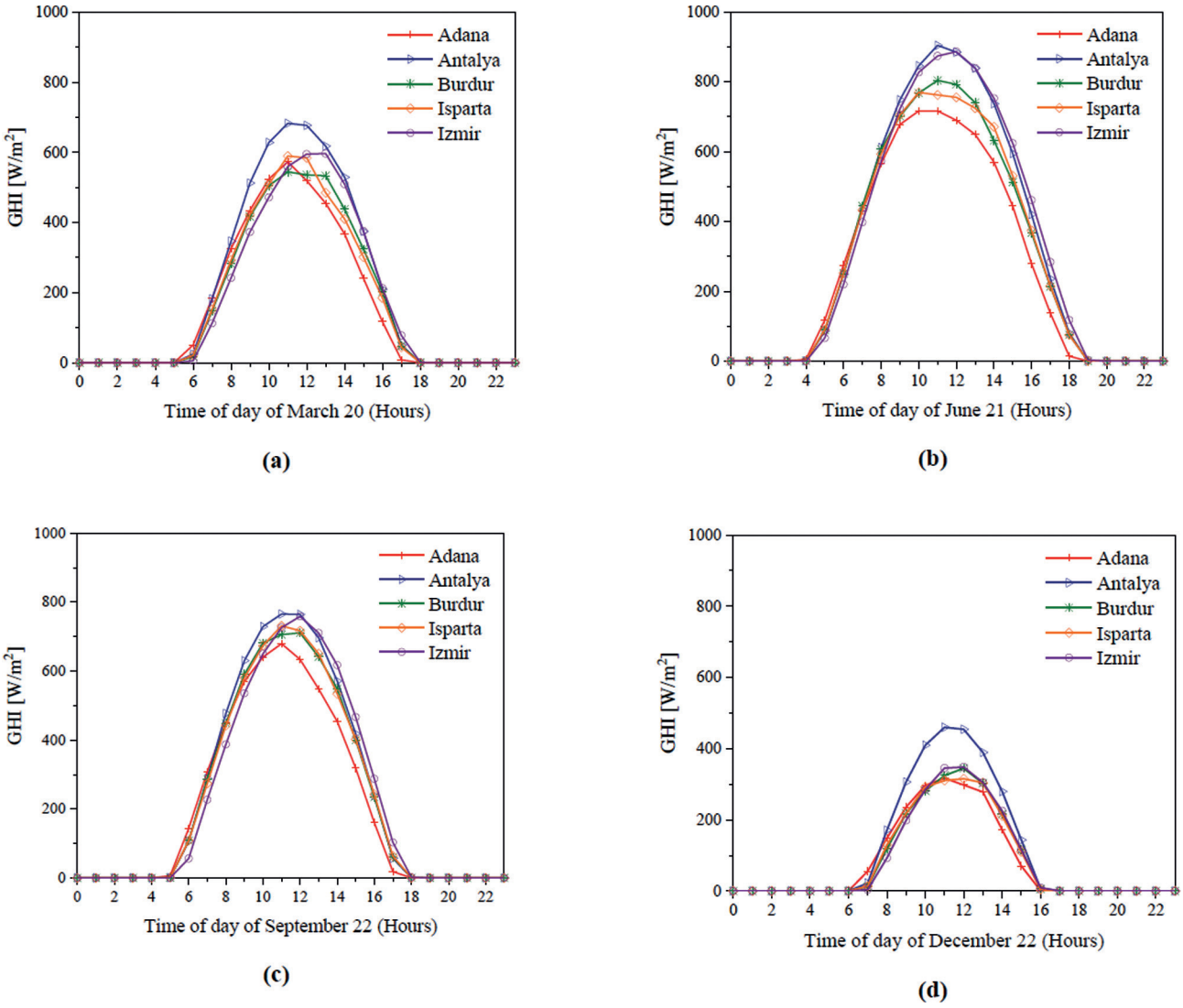

Figure 5. Global horizontal irradiation for the selected days.

their performance by varying the meteorological parameters in several Turkey regions. The large installation can be considered as a solar power plant (production industry), while the small prototype can be built as a study and research facility in laboratories for the development of this technology.

The large prototype was presented to produce an output power of 70 kW, knowing that the collector's diameter was

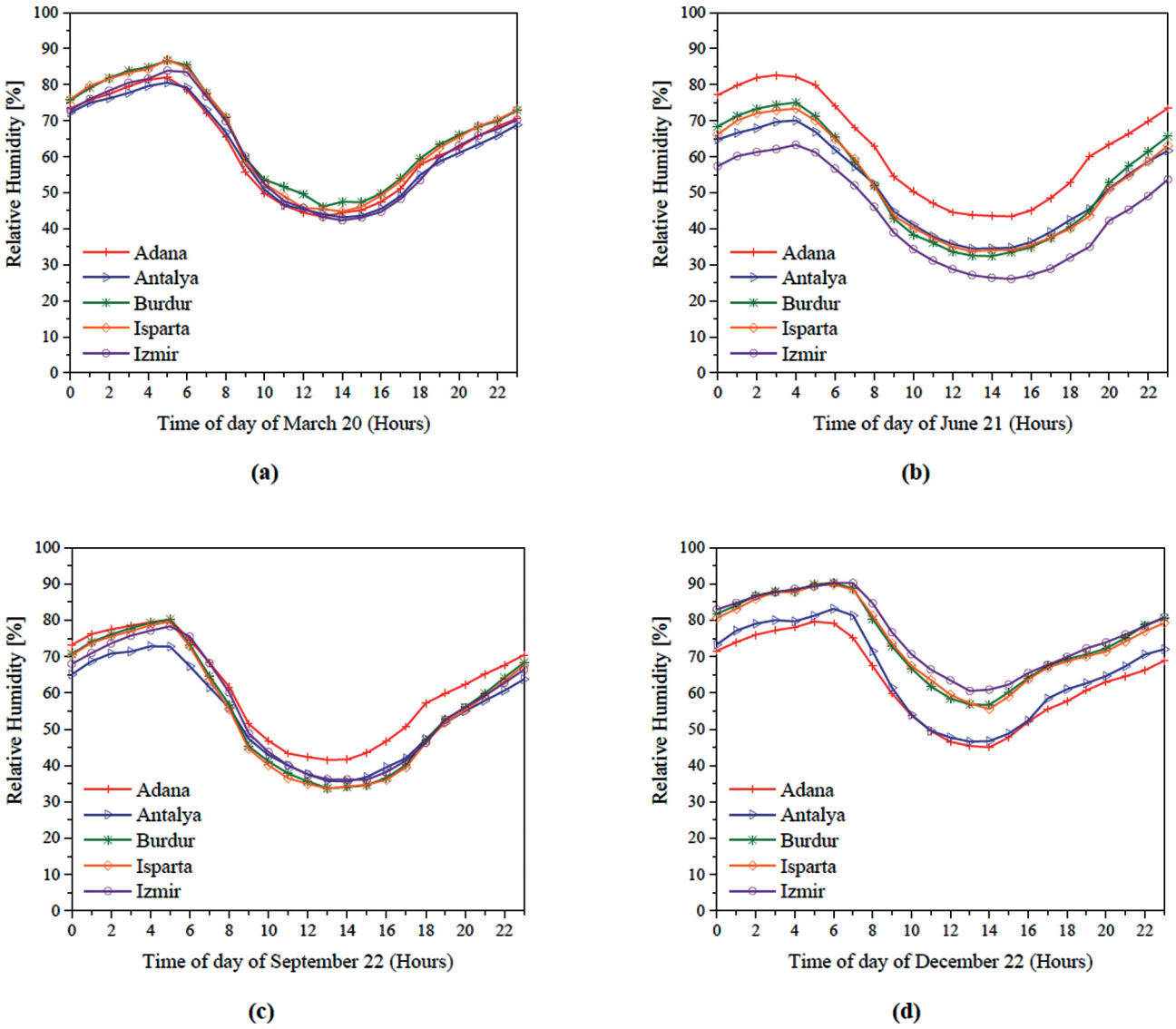

Figure 6. Relative humidity for the selected days.

300 m. The diameter and height of the chimney were 16 m and 194.6 m successfully. In comparison, the small prototype was identified to produce a power of 0.7 kW. It had the following parameters: a collector diameter of 16 m while the chimney's diameter and height are 1.2 m and 15 m.

The thermal storage system of the SCPP prototypes is composed of black tubes filled with water 16 m long for the small-scale prototype and 60 m for the large-scale one. The tubes are saturated with water only once during construction and subsequently remain closed so that no evaporation can occur, and they are placed side by side on the ground. The heat transfer between the black tubes and the water is much better than that between the surface and the deep layers of the ground (1 m), and since the heat capacity of water (4.2 kJ / kg) is much greater than that of the ground (0.71 kJ / kg). The water inside the tubes stores a large part of the solar heat and delivers it during the night when the collector's air-cools.

Table 2 illustrates a comprehensive description of the input data and parameters used in the numerical simulation. Tables 3 gives the climatic data for selected regions of Turkey.

Figures 5, 6, 7, and 8 show the average annual meteorological data needed as input for Turkey's selected regions analyzed in this study.

According to figure 5, which represents the Global Horizontal Irradiation for the 4 days selected in this study (March 20, June 21, September 22, and December 22), it is clear that the Antalya site represents the most irradiating region (GHI), followed by the Izmir region. Isparta and

Burdur have identical GHIs, mainly because they are in the same area. Last but not least, the Adana region has a low GHI compared to other regions.

On December 22, the GHI of all regions is an average of 50% less than the GHI of June 21, which can reach 900 W / m^2, while for March 20 and June 22, the GHI reaches between 600-800 W / m^2.

Figure 6 displays the relative humidity evolution versus time (hours). In general, the curves are almost identical for all the regions on March 20 and December 22. On the other hand, for June 21, we notice that Adana's region is most humid compared to the other sites, and Izmir is the least humid. Finally, we note that on December 22, Adana and Antalya are less humid regions compared to other sites.

For all the selected days of the study, we note that the humidity is less remarkable from 7:00 a.m. to 6:00 p.m., and this segment represents the production period of the power plant.

Figure 7 shows the ambient temperature evolution versus time (in hours). We notice that Burdur and Isparta's regions are the coldest for all the days selected, followed by Izmir. Antalya and Adana are the hottest regions, where they can reach 37 °C in June and September.

Figure 8 shows the wind speed evolution versus time for the selected day. Notice that the regions of Antalya

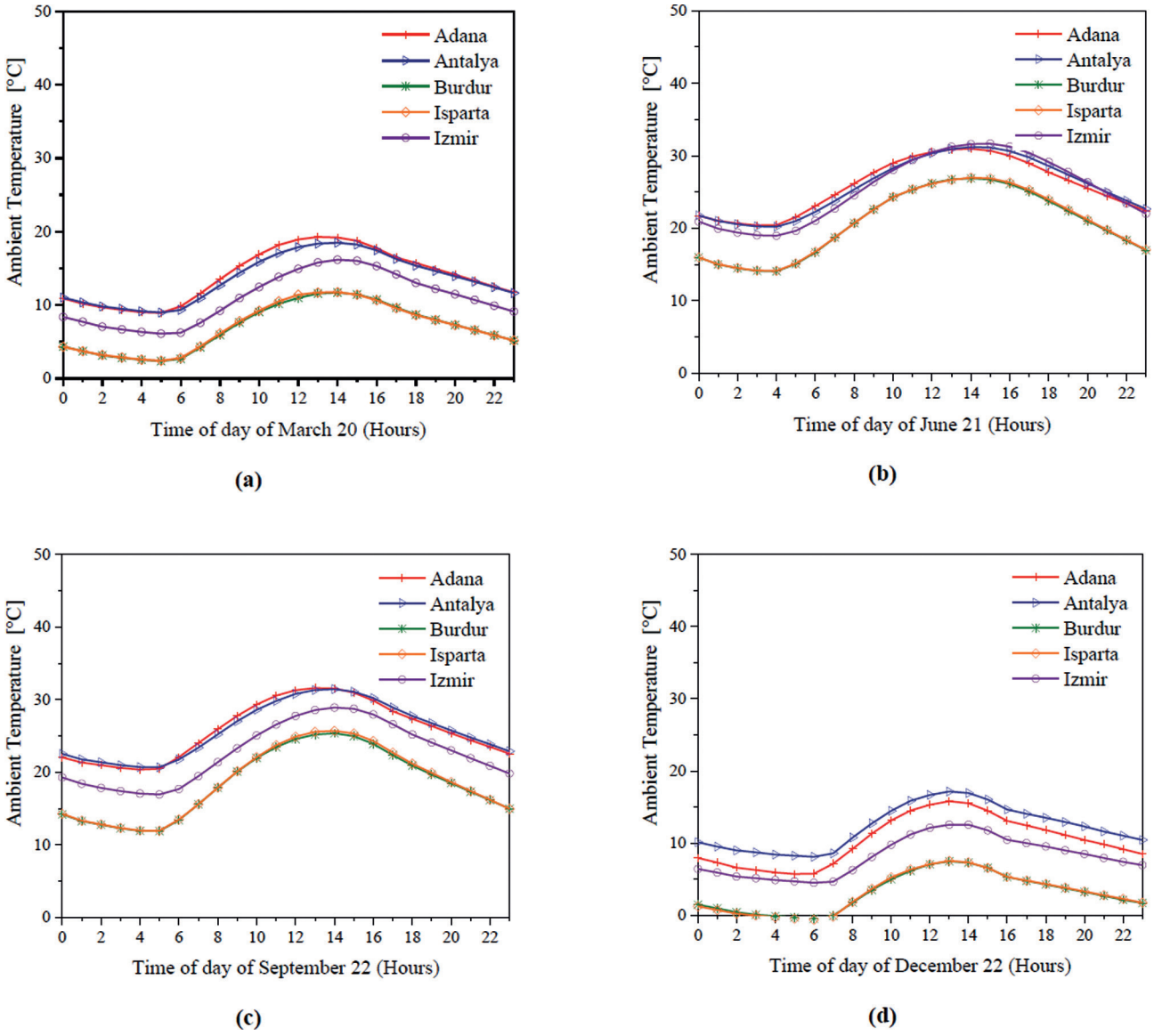

Figure 7. Ambient temperature for the selected days.

and Izmir are very windy. The wind speed exceeds 3 m/s for all the selected days and reaches 6 m/s in March and September. It is followed by Izmir, which is also a windy region. Finally, Isparta and Burdur have the lowest wind speed during all year.

Figure 9 illustrates the influence of wind speed on the output power. We have chosen the GHIs and temperatures for the day of June 22, and the Antalya region. Figure 10 represents the impact of temperature on the energy produced by Antalya's site on June 22.

According to figures 9 and 10, which represent the impact and the influence of wind speeds and temperatures on the output powers successively. Notice that these two meteorological parameters greatly influence energy production. Note that the output power decreases with the increase in wind speed (inversely proportional), and with the increase in temperature, the powers increase (proportionally). The reasons are as follows:

When the wind speed increases, the convective heat transfer coefficient also increases by directly reducing the collector's surface temperature and, therefore, the flowing air temperature. This decrease in temperature reduces the driving forces and, therefore, the system's output power.

As the ambient temperature and/or the intensity of solar radiation increases, the collector's surface temperature increases, and the flowing air temperature also increases.

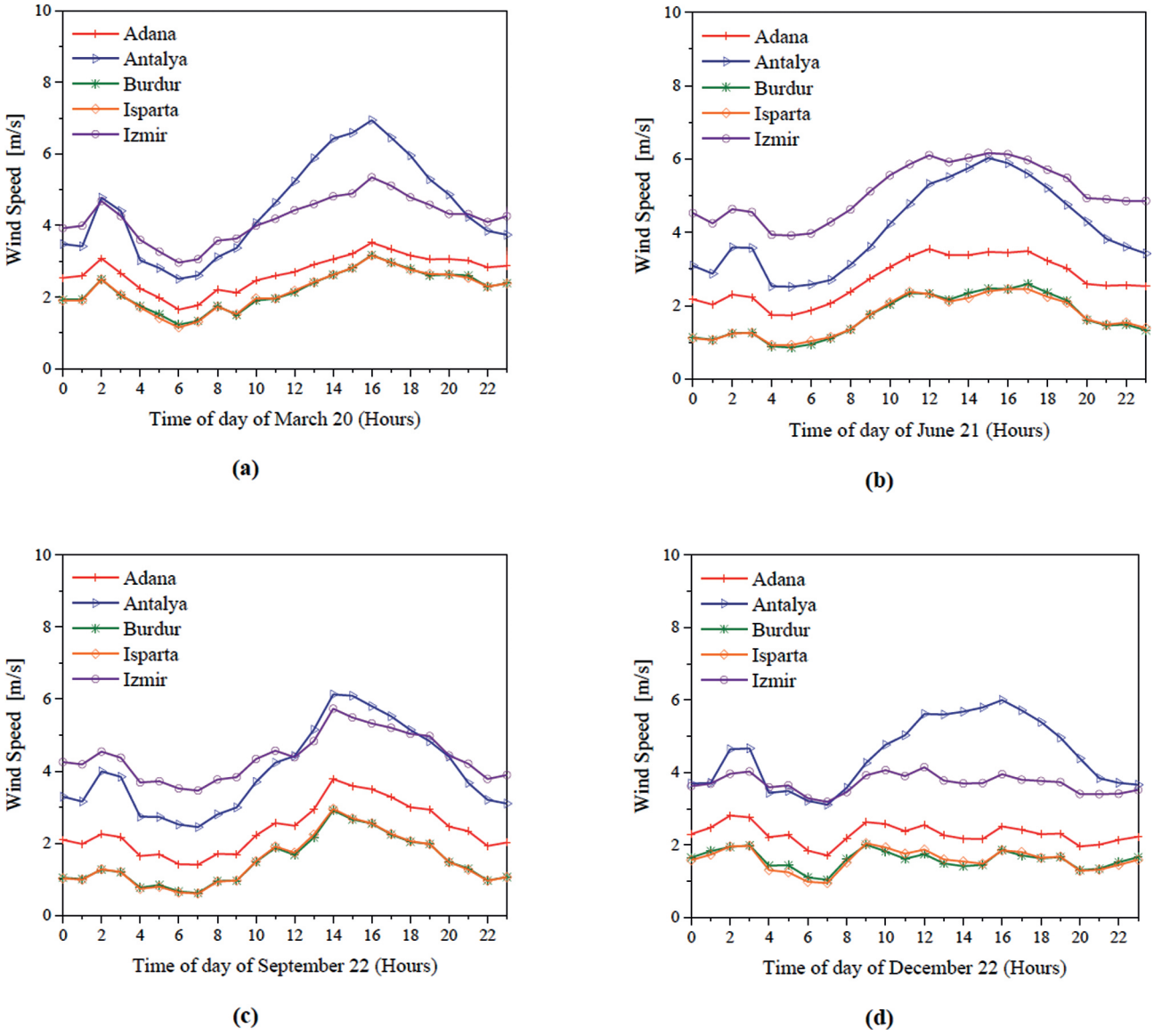

Figure 8. Wind speed for the selected days.

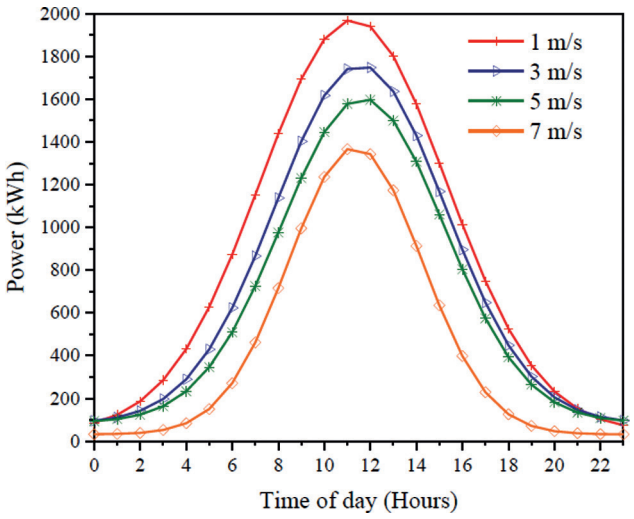

Figure 9. Influence of wind velocity on the power output.

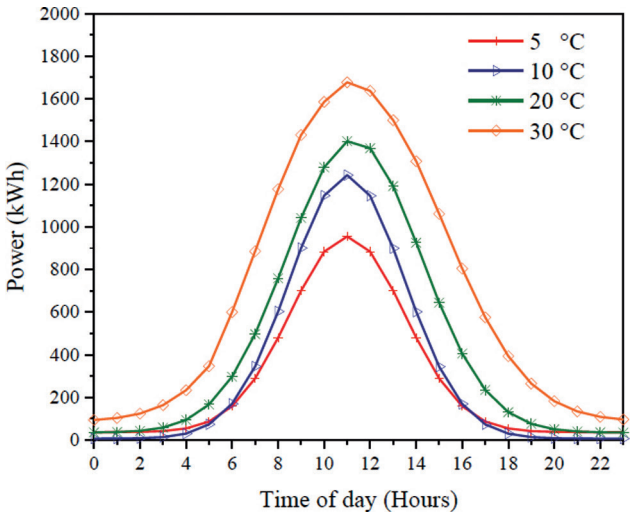

Figure 10. Influence of ambient temperature on the power output.

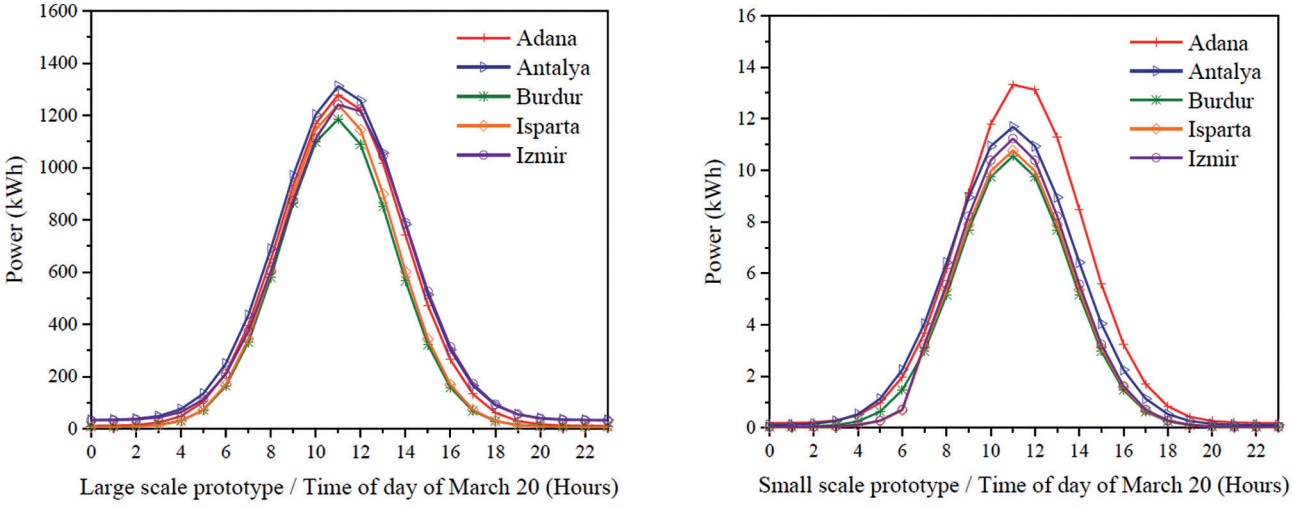

Figure 11. Output power evolution versus time for large/small scale SCPP on March 20.

This increase in temperature results in an increase in the driving forces, which directly increases power.

In the next step, we present the power produced by the large/small scale SCPP prototypes chosen for Turkey's different regions and four specific days in the year (Spring: March 20, Summer: June 21, Autumn: September 22, and Winter: December 22).

Figure 11 shows that the power generations are approximately identical because the GHI in March is almost the same in all regions, except that Antalya has a slightly higher GHI. Even though the temperature is more notable at Adana and Antalya's sites, the power output still the same. The high wind speed in Antalya and Izmir was the cause of the power reduction at these sites. The thermal storage system's effect is remarkable from 5:00 p.m. to 8:00 p.m (Low or no GHI). After this period, the SCPP stops producing energy because of the decrease (cooling) of the storage system effect.

Figure 12 illustrates the output power for the large/small scale SCPP on June 21. We notice that the Antalya and Izmir regions have the highest power output, followed by Adana and finally Isparta and Burdur. During this day,

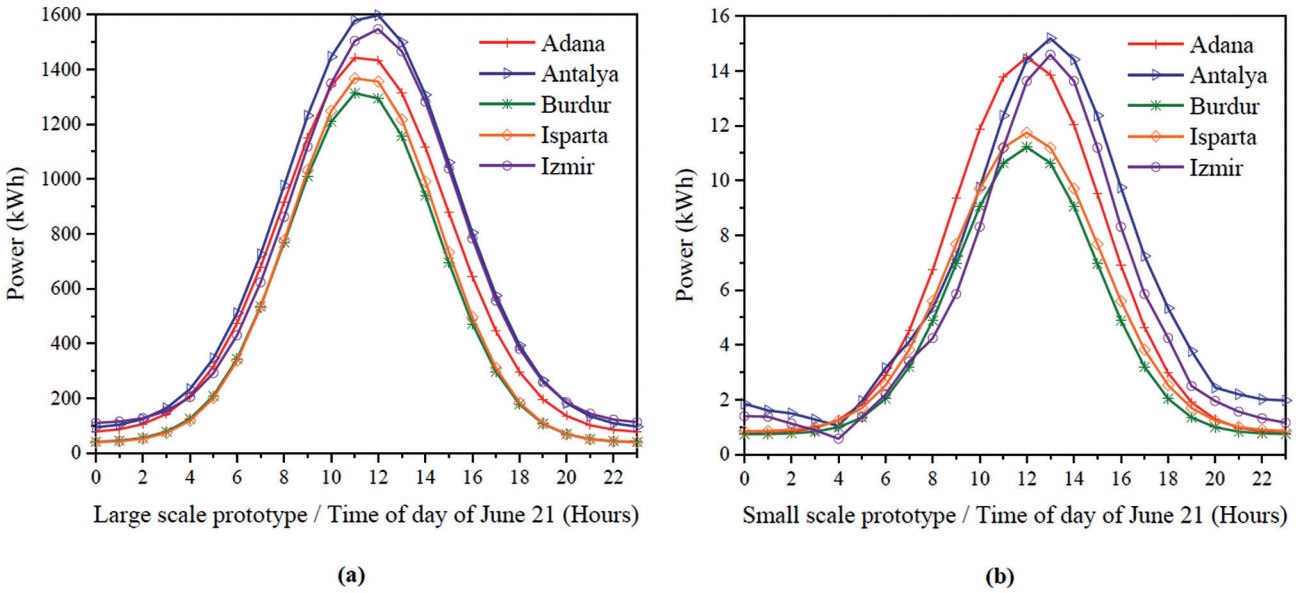

Figure 12. Output power evolution versus time for large/small scale SCPP on June 21.

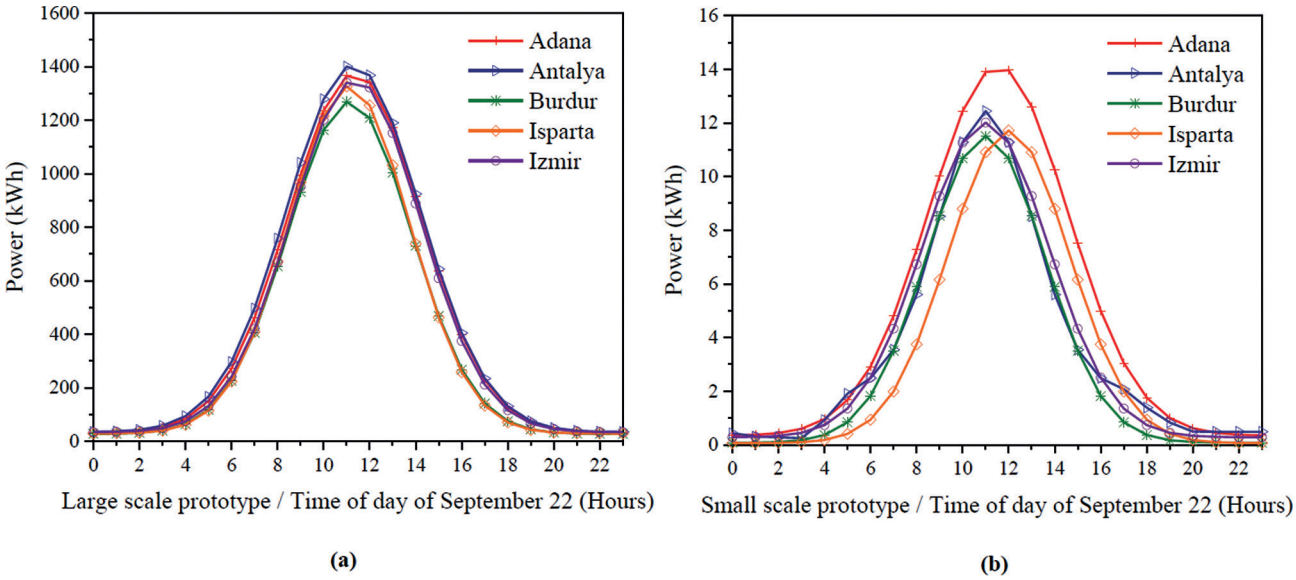

Figure 13. Output power evolution versus time for large/small scale SCPP on September 22.

GHI global solar irradiation is high in all regions except Adana; the latter has the lowest GHI but very high temperature. Although Antalya has the best GHI and the highest temperature, it does not produce much energy due to the high wind speed. It is also perceived that the power plants continue to produce energy during the night despite the GHI's absence, which explains the thermal storage system's operation.

By analyzing figure 13, we can deduce that the results are almost the same as those of March except that for this month, the duration of sunshine is high as well as the GHI, which makes the powers slightly more remarkable. We note that the Adana site has the highest power for the small-scale prototype because of the high irradiation and the high temperature. The thermal storage system is functional but less efficient than on June 22 because of the low temperature and GHI, and high wind speed.

According to figure 14, Burdur and Isparta's output power is less important than in other Turkey regions due to the low temperature (Sometimes the temperature decrease

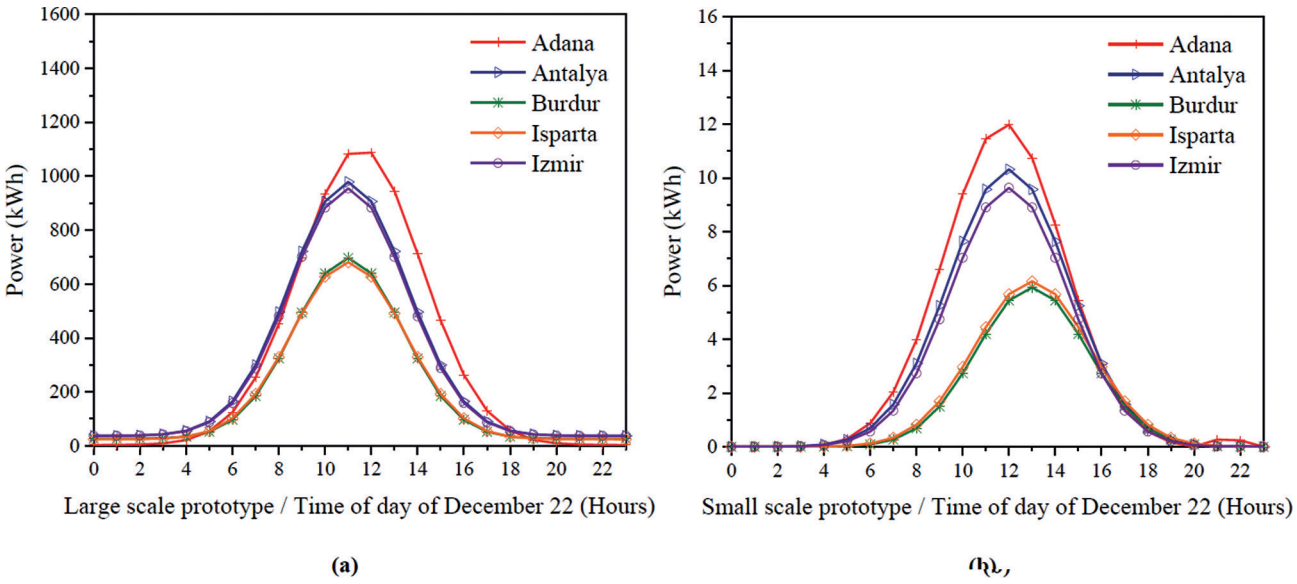

Figure 14. Output power evolution versus time for large/small scale SCPP on December 22.

Table 4. Total Annual Generated Power and Peak Power recorded for the large-scale SCPP

	Adana	Antalya	Burdur	Isparta	Izmir
Total annual generated power [kWh]	43.96E+6	46.34E+6	35.04E+6	35.92E+6	43.89E+6
Peak power recorded [kW]	60.45	66.83	54.96	57.44	64.49

Table 5. Total Annual Generated Power and Peak Power recorded for the small-scale SCPP

	Adana	Antalya	Burdur	Isparta	Izmir
Total annual generated power [kWh]	387.23E+3	439.1E+3	294.6E+3	308E+3	387.1E+3
Peak power recorded [kW]	0.61	0.63	0.47	0.49	0.61

below zero Celcius). The energy produced in the Adana site is the best due to the high temperature and low wind speed. The thermal storage system's effect on electricity production is still noticeable after midnight for the large prototype and until 10 p.m. for the small prototype but in small power. It can be deduced that the prototypes produced 50% of their nominal production.

Tables 4 and 5 represent the total annual generated power, and the peak power recorded for the solar chimney power plant SCPP large/small scale prototype. Notice that the best results are those of Antalya, followed by those of Izmir and Adana, and finally, those of Isparta and Burdur.

CONCLUSION

This study aims to estimate the solar chimney power production numerically in different Turkey regions (Adana, Antalya, Burdur, Isparta, and Izmir) by applying the Bernardes mathematical model. The theoretical calculations were performed to evaluate the production of large-scale and small-scale prototypes of SCPP. The results were validated with experimental data obtained by the SCPP prototype installed at Süleyman Demirel University in Isparta. Obtained results demonstrated that:

- Antalya's region has the best GHI and the highest temperature, which achieves a better output power.
- The Burdur and Isparta regions have the lowest results due to the low temperature and GHI compared to other regions, especially in winter.
- The wind speed influences energy production directly. Such as increasing wind speed reduces power output. The Antalya and Izmir regions support these results.
- The small-scale prototypes provided a low output power related to their dimensions. They can be used as research and validation prototypes.

Notice that the prototypes of SCPP must be installed in many countries where solar energy is important and not usable. These installations will reduce pollution, preserve

our planet, and significantly develop SCPP technology by developing thermal storage systems and suggesting hybridization with other systems for better performance.

NOMENCLATURE

A_c	Flow area, m^2
C_p	Specific heat capacity, J/kg K
d	Diameter, m
EIE	General Directorate of Electrical Power Resources Survey of Turkey
F	Force, N
g	Gravitational acceleration 9,8, m/s^2
GHI	Global horizontal irradiation
H	Height, m
h	Convective heat transfer coefficient, W/m^2 K
I	Solar irradiation, W/m^2
k	Thermal conductivity, W/ m K
Δ_{ptot}	Total pressure difference in the chimney, Pa
p	Pressure, Pa
P	Power output, W
q	Heat flux, W/m^2
R	Gas constant, J/kg K
RA	Constant gases for dry air
RV	Constant gases for water vapor
SCPP	Solar Chimney Power Plant
x	Factor of pressure drop at the turbine
T	Temperature, K
t	Time, s or thickness, m
v	Radial velocity component, m/s
vc	Vertical velocity component, m/s
w_{tot}	Velocity obtained neglecting friction losses, m/s
z	Vertical coordinate, m

Greek symbols

α	Absorptivity or coefficient or angle, Radians or degrees
ϵ	Emissivity
η_t	Mechanical efficiency
θ	Angle radians, Rad
ρ	Density, kg/m^3
σ	Boltzmann's constant, $5.67 \times 10–8$ W/m^2 K^4
τ	Shear stress, Pa, or transmissivity
φ	Relative humidity

Subscripts

a	Ambient air
b	Beam
bw	Bracing wheel
c	Collector
d	Diffuse
e	Effective or extinction
g	Ground
gr	Ground to collector roof
gh	Ground to air under collector roof
h	Horizontal surface or air under collector roof or hydraulic
r	Roof or radial
ra	Collector roof to ambient air
rh	Collector roof to air under collector roof
rs	Collector roof to the sky
sky	Sky
supports	Collector roof supports

AUTHORSHIP CONTRIBUTIONS

Authors equally contributed to this work.

DATA AVAILABILITY STATEMENT

The authors confirm that the data that supports the findings of this study are available within the article. Raw data that support the finding of this study are available from the corresponding author, upon reasonable request.

CONFLICT OF INTEREST

The author declared no potential conflicts of interest with respect to the research, authorship, and/or publication of this article.

ETHICS

There are no ethical issues with the publication of this manuscript.

REFERENCES

[1] Kasaeian AB, Molana SH, Rahmani K, Wen D. A review on solar chimney systems. Renew Sustain Energy Rev 2017;67:954–987. [CrossRef]

[2] Fluri TP, Pretorius JP, Van Dyk C, Von Backström TW, Kröger DG, Van Zijl GPAG. Cost Analysis of Solar Chimney Power Plants. Conference: EUROSUN 2006, 2006, Glasgow, Scotland.

[3] Pasumarthi N, Sherif SA. Experimental and theoretical performance of a demonstration solar chimney model. Part I: Mathematical model development. Int J Energy Res 1998;22:277–288. [CrossRef]
[4] Haaf W. Solar chimneys, part ii: preliminary test results from the manzanares pilot plant. Int J Sol Energy 1984;2:141–161. [CrossRef]
[5] Schlaich J. Tension structures for solar electricity generation. Eng Struct 1999;21:658–668. [CrossRef]
[6] Haaf W, Friedrich K, Mayr G, Schlaich J. Solar chimneys. Part I: Principle and construction of the pilot plant in Manzanares. Int J Sustain Energy 1983;2:3–20. [CrossRef]
[7] Kulunk H. A Prototype Solar Convection Chimney Operated under Izmit Conditions. TN Veiroglu, Proceedings of the 7th Miami International Conference on Alternative Energy Sources 1985;162.
[8] Sherif SA, Pasumarthi N, Harker RA, Brinen GH. Performance of a demonstration solar chimney model for power generation. Final Technical Report No.UFME/SEECL-9507, 1995. Solar Energy and Energy Conversion Laboratory, Department of Mechanical Engineering, University of Florida, Gainesville.
[9] Zhou XP, Yang JK, Xiao B, Hou GX. Experimental study of the temperature field in a solar chimney power setup. Appl Therm Eng 2007;27:2044–2050. [CrossRef]
[10] Ketlogetswe C, Fiszdon JK, Seabe O. Solar Chimney Power Generation Project - The Case for Botswana. Int J Renew Sustain Energy Rev 2008;12:2005–2012. [CrossRef]
[11] Ferreira AG, Maia CB, Cortez MFB, Valle RM. Technical Feasibility Assessment of a Solar Chimney for Food Drying. Sol Energy 2008;82:198–200. [CrossRef]
[12] Koyun A, Üçgül I, Acar M, Şenol R, Güneş R. Bacası sisteminin termal özet dizaynı. Tesisat Mülhendisliği Dergisi 2007;98:45–50.
[13] Golder K. Combined Solar Pond and Solar Chimney. Final year Mechanical Engineering Project. School of Aerospace, Mechanical and Manufacturing Engineering, Bundoora Campus, RMIT University, Melbourne, Australia; 2003.
[14] Mehla N, Makade R, Thakur NS. Experimental analysis of a velocity field using variable chimney diameter for solar updraft tower. Int J Eng Sci Technol 2011; 3:3167–3171.
[15] Bugutekin A. Effect of the collector diameter on solar chimney power plants. Energy Educ Sci Technol Part A Energy 2011, Sci Res 2011;27:155–168.
[16] Al-Dabbas MA. The first pilot demonstration: solar updraft tower power plant in Jordan. Int J Sustain Energy 2012;31:399–410. [CrossRef]
[17] Chappell RD, Congdon MJ, French JJ. Design, construction, and testing of a small-scale solar chimney for nomadic herdsmen. In: Proceedings of the ASME 2012 6th international conference on energy sustainability. San Diego, California, USA, 2012. [CrossRef]
[18] Nasraoui H, Driss Z, Kchaou1 H. Effect of the chimney design on the thermal characteristics in solar chimney power plant. J Therm Anal Calorim 2020;140:2721–2732. [CrossRef]
[19] Azizi A, Tahri T, Sellami MH, Segni L, Belakroum R, Loudiyie K. Solar Chimney Power Generation in the South of Algeria: Experimental Study. Springer Proceedings in Energy 2019;135–140. [CrossRef]
[20] Padki MM, Sherif SA. Solar Chimneys for Medium-to-Large Scale Power Generation. Proceedings of the Manila International Symposium on the Development and Management of Energy Resources, Volume 1, Manila, Philippines 1989; 432–443, January 26–28.
[21] Schlaich J, Bergermann R, Schiel W, Weinrebe G. Design of commercial solar updraft tower systems-utilization of solar induced convective flows for power generation. J Sol Energy Eng 2005;127:117–124. [CrossRef]
[22] Chergui T, Larbi S, Bouhdjar A, Gahgah M. Influence of the Thermo hydrodynamic Aspect of Fluid Flow on the Performance Analysis of a Solar Chimney Power Plant. In: Proceedings of the World Renewable Energy Congress, Asia, 2009.
[23] Semai H, Bouhdjar A, Larbi S. Solar Chimney Power Plant with Heat Storage System Performance Analysis in South Region of Algeria. 2015 3rd International Renewable and Sustainable Energy Conference (IRSEC);2015:1–6. [CrossRef]
[24] Ikhlef K, Larbi S. Energy performance analysis of a solar chimney power plant with and without thermal storage system. International Journal of Control, Energy and Electrical Engineering 2019;11:1–7.
[25] Padki MM, Sherif, SA. A mathematical model for solar chimneys. Proceedings of the International Renewable Energy Conference, in Renewable Energy: Research and Applications, Vol. 1, M.S. Audi (Ed.), University of Jordan, Faculty of Engineering and Technology, Amman, Jordan, 289–294, June 22–26, 1992.
[26] Li JY, Guo PH, Wang Y. Annual performance analysis of the solar chimney power plant in Sinkiang, China. Energy Conversion and Management 2014;87:392–399.
[27] Dos Santos Bernardes MA, Vob A, Weinrebe G. Thermal and technical analyses of solar chimneys. Sol Energy 2003;75:511–524. [CrossRef]
[28] Dos Santos Bernardes MA, Valle R, Cortez MFB. Numerical Analysis of Natural Laminar Convection in a Radial Solar Heater. Int J Therm Sci 1999;38:42–50. [CrossRef]

[29] Zhou XP, Yang JK, Xiao B, Long F. Numerical Study of a Solar Chimney Thermal Power Setup Using Turbulent Model. J Energy Inst 2008;81:86–91. [CrossRef]

[30] Maia CB, Ferreira AG, Valle RM, Cortez MFB. Theoretical evaluation of the influence of geometric parameters and materials on the behavior of the air flow in a solar chimney. Comput Fluids 2009; 38:625–636.

[31] Chergui T, Larbi S, Bouhdjar A. Thermo-hydrodynamic aspect analysis of flows in solar chimney power plants - a case study. Renew Sustain Energy Rev 2010;14:1410–1418. [CrossRef]

[32] Tayebi T, Djezzar M. Effect of varying ambient temperature and solar radiation on the flow in a solar chimney collector. Int J Smart Grid Clean Energy 2016;5:16–23. [CrossRef]

[33] Zhou X, Xu Y, Zhang F. Evaluation of effect of diurnal ambient temperature range on solar chimney power plant performance. Int J Heat Mass Transf 2017;115:398–405. [CrossRef]

[34] Das P, Chandramohan VP. 3D numerical study on estimating flow and performance parameters of solar updraft tower (SUT) plant: Impact of divergent angle of chimney, ambient temperature, solar flux and turbine efficiency. J Clean Prod 2020;256:120353. [CrossRef]

[35] Dos Santos Bernardes MA. Technische, ökonomische und ökologische Analyse von Aufwindkraftwerken. PhD Thesis, Stuttgart University, Stuttgart, 2004. (in Deutsch)

[36] Dos Santos Bernardes MA. Solar Chimney Power Plants–Developments and Advancements. Sol Energy 2010:978–953. (in Brasil)

[37] Dos Santos Bernardes MA, Zhou X. Strategies for solar updraft tower power plants control subject to adverse solar radiance conditions. Sol Energy 2013;98:34–41. [CrossRef]

[38] Pretorius JP. Solar tower power plant performance characteristics. Thesis presented at the University of Stellenbosch; April 2004.

[39] Dos Santos Bernardes MA. Preliminary stability analysis of the convective symmetric converging flow between two nearly parallel stationary disks similar to a Solar Updraft Power Plant collector. Sol Energy 2017 141:297–302. [CrossRef]

[40] Dos Santos Bernardes MA. Correlations for the symmetric converging flow and heat transfer between two nearly parallel stationary disks similar to a solar updraft power plant collector. Sol Energy 2017;146:309–318. [CrossRef]

[41] Egolf PW, Frei B, Furter R. Thermodynamics of moist air: contribution to error estimates. Appl Therm Eng 2000;20:1–19. [CrossRef]

[42] ASHRAE Fundamentals Handbook (SI), Psychrometrics, Chapter 6.8: Moist Air; 2001.

[43] Marco-Bernardes / SUPP-Java. Open source program. Github. https://github.com/Marco-Bernardes/SUPP-Java.

[44] Koyun A, Ucgul I, Acar M. Development of a computer program for solar chimney. Energy Education Science and Technology Part A: Energy Science and Research 2013;31:175–186.

[45] Yabuz ZR. Güneş bacasında konstrüktif iyileştirme çalişmalari ve performans artirici yöntemlerin araştirilmasi. Master Thesis, Makina Mühendisliği Anabilim Dali, Isparta, 2009. (in Turkish)